Experimental Investigation on Uniaxial Unconfined Compressive Properties of Ice on Asphalt Pavement Surface

Wei Luo[1,2], Hancheng Dan[3]*, Runzhong Zeng[1], Yao Rong[2] and Dian Xie[1]

[1] School of Civil Engineering and Architecture, East China Jiaotong University, Nanchang, China, [2] Jiangxi Transportation Institute, Nanchang, China, [3] School of Civil Engineering, Central South University, Changsha, China

Mechanical deicing is a method to remove the ice on the pavement surface, and the ice strength directly affects the difficulty and effectiveness of the mechanical deicing. This paper aims to investigate the compression strength of ice to facilitate the deicing equipment to crush ice. In this paper, a large-scale freezing laboratory is employed to simulate low-temperature environment, and the uniaxial unconfined compressive tests of artificial freshwater ice under different temperature conditions are carried out through the uniaxial loading system. The compressive strength and modulus of ice are obtained when the substrate is asphalt pavement. The test result shows that the ice compressive strength and modulus respectively distribute from 0.36 to 3.67 MPa and 11.7 to 359.1 MPa when ice temperature varies from −0.7 to −7.5°C. The relations between ice temperature and compressive strength are approximately in a linear manner, while the relation of compressive modulus and ice temperature shows good power function and exponential relationships, respectively, when ice temperature ranges from −8 to −5°C and from −5 to 0°C. Furthermore, the failure mechanism of ice under relatively lower temperature is due to the development of cut-through cracks inside the ice. The failure mode divides into shear failure and ductile failure and the failure ice is mainly composed of large ice strips and bulks. For the ice with relatively higher temperature especially the ice close to melting point temperature, the ice failure mode is compressive and ductile, and the failure ice is mainly composed of granular ice crystals.

Keywords: ice, compressive strength, compressive modulus, asphalt pavement, failure mode

INTRODUCTION

The ice formed on the surface of civil structures exerts adverse impacts on the engineering construction and its normal use (Hanbali, 1994; Dan et al., 2019a,b). It is well known that the wet asphalt pavement is more likely to be frozen in the low-temperature environment especially in moist mountain area (Dan et al., 2014, 2020a). The area in western China often suffers from freezing rain during the winter, and ice on the asphalt pavement reduces the pavement skid resistance and subsequently endangers the traffic safety (Gustafson, 1982; Zhu et al., 2012; Dan et al., 2020c).

For instance, a massive ice disaster occurred in western China. Thereinto, the Guizhou province suffers from the most severe ice disaster during the winter in 2008 (Chen et al., 2008). The ice thickness reaches 20 cm and caused many serious traffic accidents. Accordingly, the ice pavement problems with respect to ice warning and deicing should be taken seriously (Dan et al., 2014). Currently, many technologies were developed to deice (Croutch and Harttey, 1992; Petrenko, 1999; Sarkar and Farzaneh, 2009), including the mechanical deicing technology (SHRP, 1994; Taggart et al., 2002; Dan et al., 2020b). In general, the ice strength directly affects the difficulty and effectiveness of the mechanical deicing (Oksanen, 1983; SHRP, 1994; Tan, 2008). So far, there are few studies on the ice strength when the substrate is asphalt pavement. Nonetheless, relatively more researches have presented to measure the ice strength under certain conditions in the other research fields (Gow and Williamson, 1972; Haynes and Mellor, 1977; Sodhi, 2001; Marion and Jakubowski, 2004; Kärnä et al., 2010).

Gow and Williamson (1972) used a novel technique to measure the linear compressibility of ice at relatively low pressures. A mean linear compressibility of 3.7 Mb^{-1} was obtained at $-10°C$. Haynes and Mellor (1977) developed a simple but accurate method for making lateral restraint compressive strength tests on right circular cylinders. Sodhi (2001) conducted small-scale indentation tests with compliant structures and freshwater ice sheets. The results of the present study with compliant structures show that there is ductile deformation of ice at low indentation speeds and continuous brittle crushing at high indentation speeds. Kärnä and Jochmarm (2003) discussed some of failure modes observed while different ice formations were acting on the lighthouse, and the details of the bending failure mode and ice crushing were described. Marion and Jakubowski (2004) presented a new model for estimating the compressibility of ice based on chemical thermodynamic principles and compared these model results with previous work. Their estimate of ice compressibility demonstrated significant temperature dependence. Yurtseven and Kilit (2009) calculated the isothermal compressibility using the experimental data for the heat expansion of ice I in the pre-melting region. By analyzing the data at various pressures, compressibility is predicted as functions of temperature and pressure near the melting point in ice I. Kärnä et al. (2010) conducted a study of dynamic interaction processes between a drifting ice sheet and a conical offshore structure. They used the conventional test techniques to study the ice failure process due to upward and downward breaking cones.

These researchers have made essential contributions to understanding ice strength and modulus under various conditions, however, most of them focus on the case that ice temperature is below $-10°C$, and few researches were conducted when the ice temperature is above $-10°C$. The Guizhou province locates in the south of mid-latitude region of the northern hemisphere, and the minimum air temperature during winter is above $-10°C$. Thus, the temperature of ice formed on the pavement is basically not below $-10°C$ (Chen et al., 2008). Therefore, this paper aims to investigate the compression strength of ice to facilitate the deicing equipment to crush ice, and the laboratory study is carried out to understand the compressive properties of ice on asphalt pavement above $-10°C$. After removing the covered ice layer, the performance of anti-skid resistance is improved and the traffic accidents is reduced accordingly.

EXPERIMENTAL PROGRAM

The factors that influence mechanical property of ice are various (e.g., the ice temperature, load speed, specimen size, and the substrate type). In this paper, we mainly focus on the study on the ice compressive strength and modulus for various ice temperatures when the substrate is asphalt pavement. The current researchers carried out some studies on the compressive failure mode of ice under different loading speeds (Sinha, 1981; Timco and Frederking, 1982; Weertman, 1983; Schulson, 2001; Petrovic, 2003; Montagnat et al., 2014). It can be found that the ice failure process under fast loading is complex with uncertainty, and the ice strength and the compressive modulus are not exact to determine (Schulson, 2001). Therefore, the research emphasizes the case of slow loading speed (the quasi static loading) in this paper.

Specimen Production

The schematic diagram of test specimen is shown in **Figure 1**. The Marshall specimen (compacted and molded asphalt mixture) is a substrate with rough surface on which the ice is formed under a low-temperature environment in order to ensure the ice specimen cannot move during the compression process. The asphalt mixture is AC-13, of which the mean texture depth is 0.75 mm. The impermeable adhesive tape twines around on the top of the Marshall Specimen and the height of protruding over the top is about 40 mm (**Figure 1**). Therefore, it forms a cup shape and is watertight. Then, the "cup shape specimen" is filled with fresh water and put into freezing laboratory under a low-temperature environment for enough time and the fresh water will be frozen. The ice specimen is columnar and Ice-1h, which is of the hexagonal crystal structure. The crystal growth direction is perpendicular to the substrate surface. The following steps are to peel off the adhesive tape and smooth ice surface with special polisher (because the surface of ice is generally concave–convex, it affects contact performance between ice surface and loading platen) (**Figure 1**). Then, the height of the ice cylinder is measured with a Vernier caliper and the ice temperature is tested with a platinum temperature sensor.

It should be pointed out that according to the field investigation and research results, the road surface can form the thickest of about 20 cm ice in the road section of severe icing in Guizhou Province, and the greatest thickness of ice is about 4 cm. Generally, the method of mechanical deicing will be adopted, and the strength of ice has a great influence on the selection of mechanical deicing equipment. Therefore, the 40 mm depth ice is chosen for testing.

Equipment and Scheme

Ice is essentially formed in a wet and low-temperature environment. The large-scale freezing laboratory is constructed

for simulating this kind of environment. The air temperature, rainfall, wind speed, and pavement temperature can be controlled. The experimental model of pavement is filled with building materials (asphalt mixture), and it is constructed in the freezing laboratory and subjected to low temperature and wet conditions.

The schematic diagram of test platform is shown in **Figure 2**. The specimen used to be compressed is placed on a metal cushion, which is put on an asphalt pavement surface. The thickness of the metal cushion depends on the distance between the ice specimen and the loading platen. In order to ensure the uniformity of force applied on the ice top, the centers of loading platen and ice top should be in a line. Then, the uniaxial loading system will work and the loading platen will increasingly move toward the ice specimen until it makes contact with the ice top surface. The movement speed of the loading platen can be controlled and changed through a computer system. As load

increases, the ice on the Marshall specimen will be broken down and lose strength.

Experimental Process
Test Preparation

Before conducting the ice compressive test, the loading–unloading performance is tested. The loading–unloading curve is plotted in **Figure 3**. It can be seen from the diagram that the maximum load value is about 100 kN, and the system will unload if load is beyond 100 kN. In addition, the compressive strength under the unconfined condition is also tested for the purpose of estimating the failure load of the Marshall specimen. For instance, the failure load test curve of the Marshall specimen for −4°C is illustrated in **Figure 4**. It can be seen that the peak load (failure load) value is about 90 kN and the compressive strength is about 11 MPa (the ratio of the peak
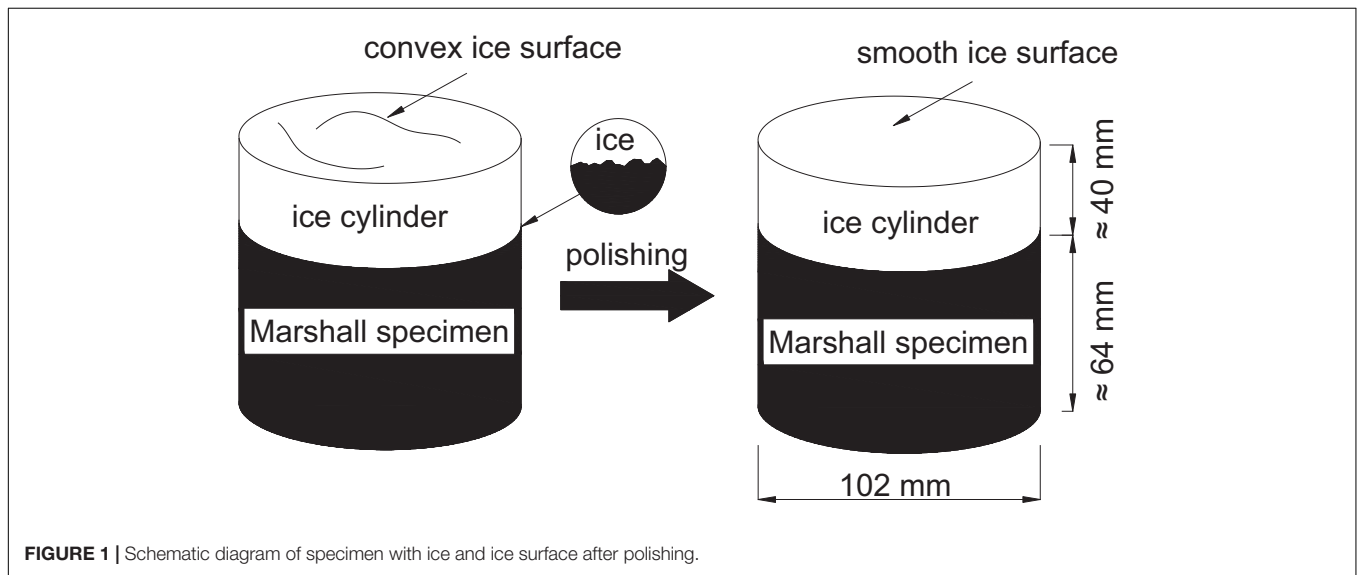

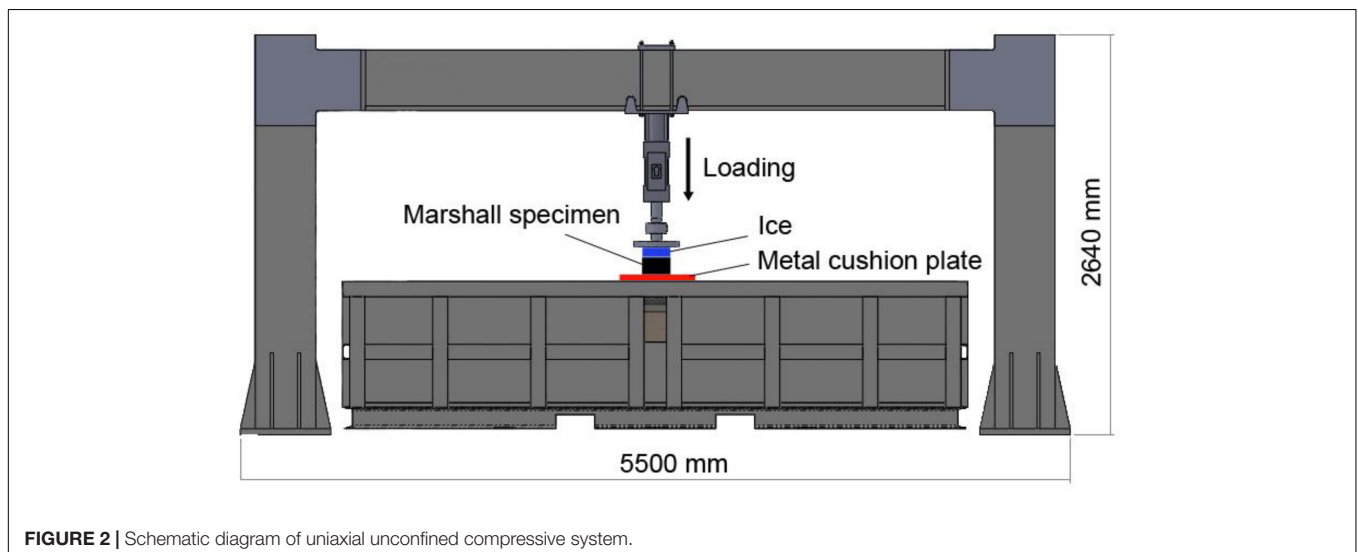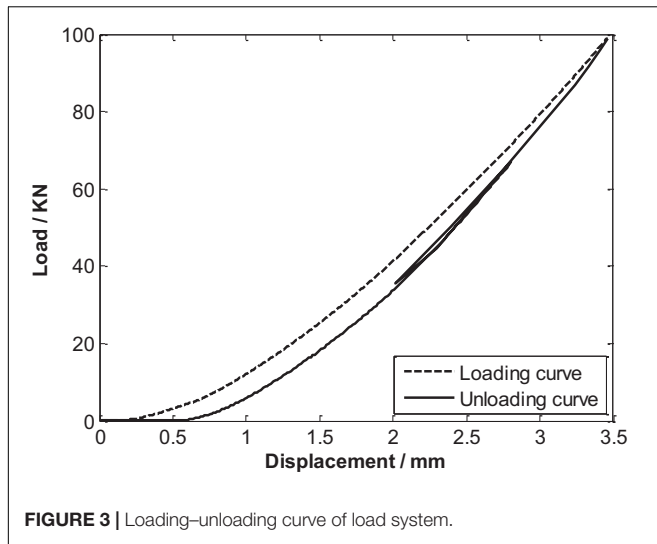**FIGURE 1 |** Schematic diagram of specimen with ice and ice surface after polishing.

FIGURE 2 | Schematic diagram of uniaxial unconfined compressive system.

FIGURE 3 | Loading–unloading curve of load system.

the deformation of the Marshall specimens under various temperature conditions.
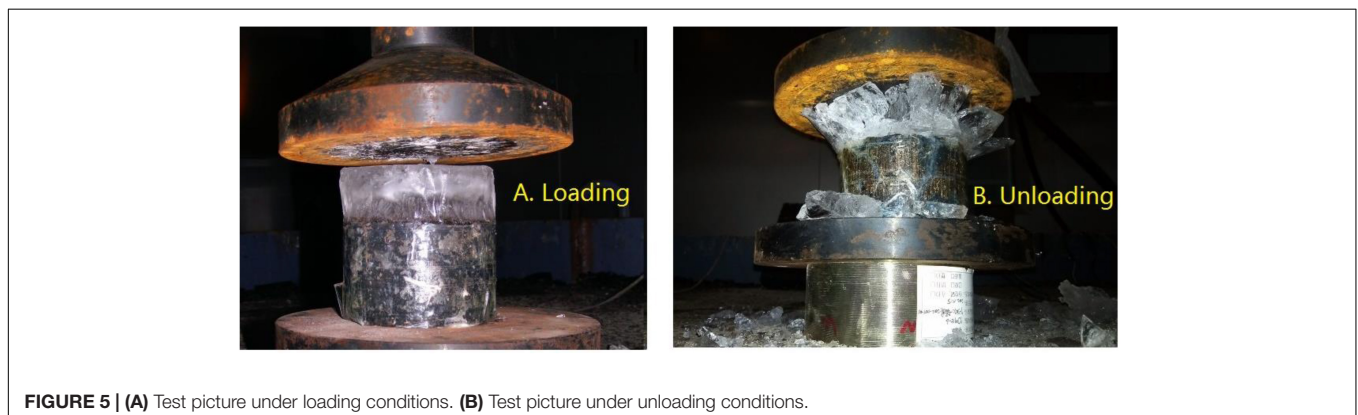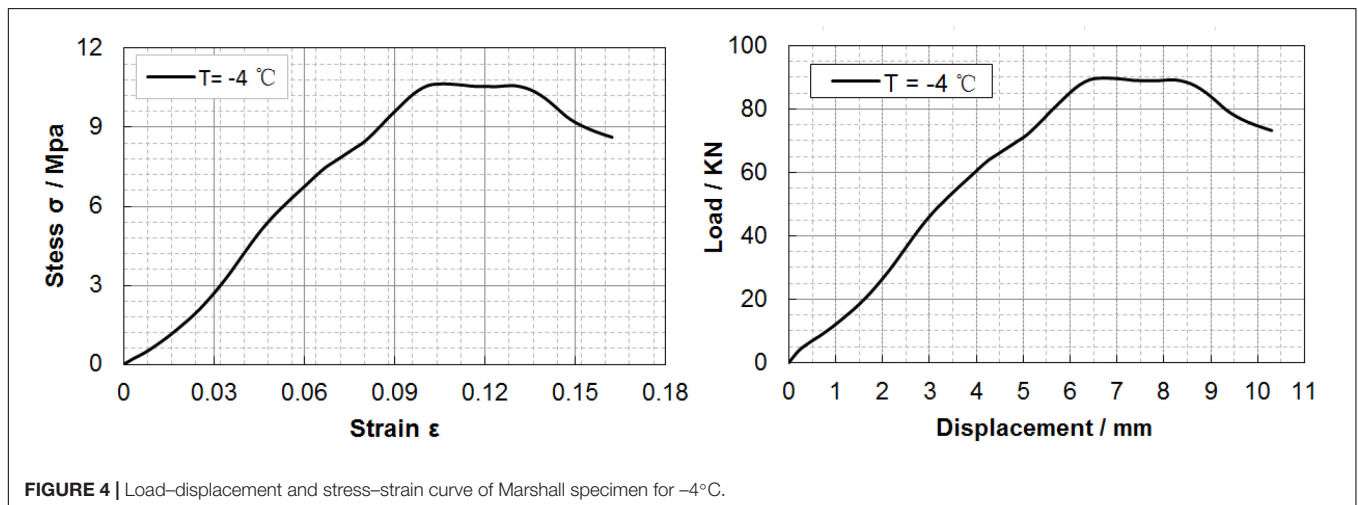
Test Procedures

The test specimen with ice is placed on the test platform (**Figure 5A**), and it should be ensured that the test temperature is close to the ice temperature (the temperature change of ice can be neglected). Then, the movement of loading platen is controlled by the computer system and the speed is specified as 2 mm/min (the strain ratio is $8.33 \times 10^{-4} \text{ s}^{-1}$) (Zhang L. M. et al., 2009; Zhang et al., 2011). During the test, the computer controlling system can automatically record load and displacement simultaneously. After stop loading, the loading platen is uplifted and separated from the ice surface (**Figure 5B**). Accordingly, the loading–unloading process is accomplished. The test cases depend on the ice temperatures from Zhang et al. −10 to 0°C, which is accurately measured by the temperature sensor.

RESULTS AND DISCUSSION

Test Results of Ice Strength

According to the experimental scheme, uniaxial unconfined compressive strength failure tests of ice are carried out under

load to the contact area). Therefore, the effective test needs the precondition that the failure load and failure strength of ice should be lower than 90 kN and 11 MPa, respectively. Moreover, several compressive tests are conducted for testing

FIGURE 4 | Load–displacement and stress–strain curve of Marshall specimen for –4°C.

FIGURE 5 | **(A)** Test picture under loading conditions. **(B)** Test picture under unloading conditions.
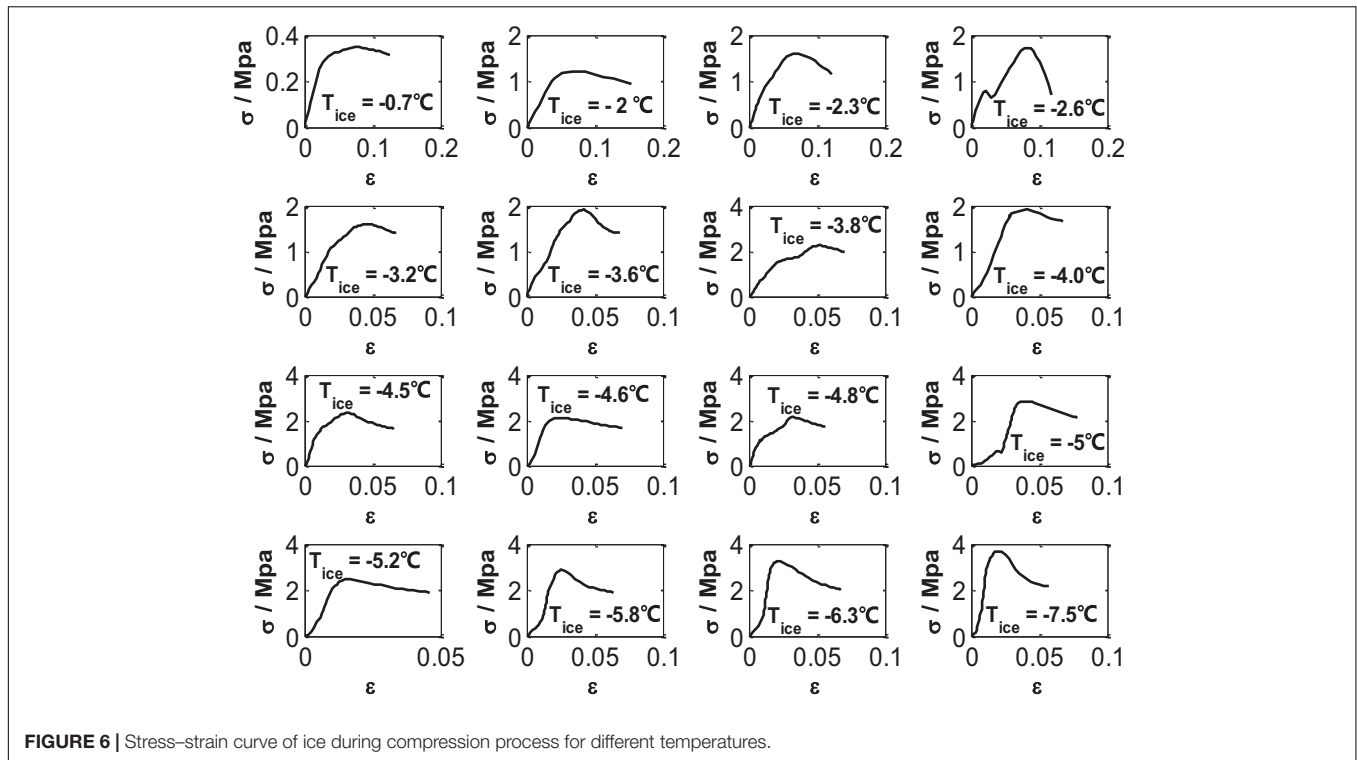
FIGURE 6 | Stress–strain curve of ice during compression process for different temperatures.
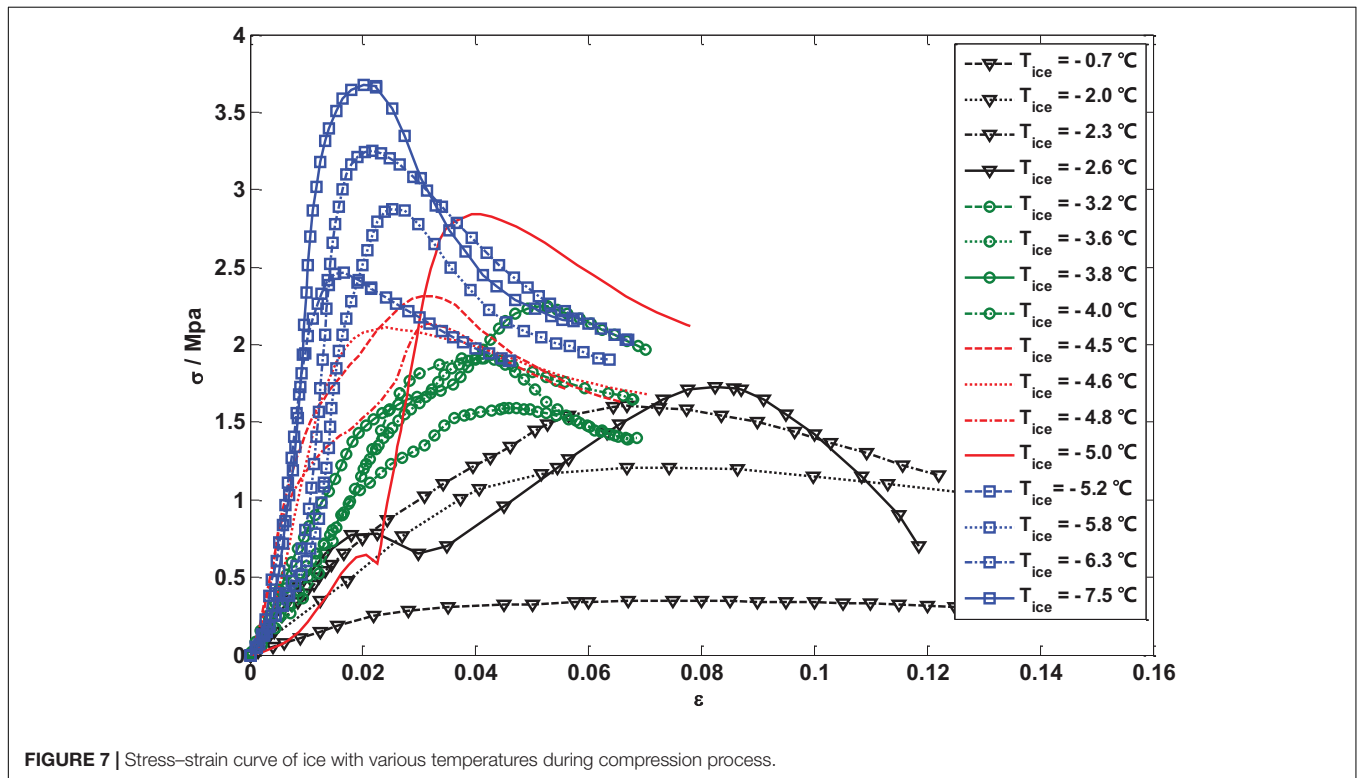

FIGURE 7 | Stress–strain curve of ice with various temperatures during compression process.

different ice temperatures, and the stress–strain curves are also obtained, which are shown in **Figures 6**, **7**. The peak value of stress is the compressive strength and the gradient of the linear segment in the stress–stain curve is compressive modulus.

The test results are aggregated in **Table 1**. It can be seen from **Figure 6** that the obvious peak value of stress can be observed in the sub-figures. Typically, the stress grows up with the strain increase and then falls down after the stress reaches its peak.

Furthermore, it can be seen from **Table 1** that all the peak load values do not exceed the critical load (the load when the Marshall specimen is failure).

Figure 7 shows various positions that peak stress occurs in the stress–strain curves when ice temperatures are different. It indicates that the deformation properties of ice for various temperatures are not the same. The relationship between ice temperature and strain corresponding to the peak stress occurrence (i.e., failure strain of ice) is shown in **Figure 8**. Overall, the strain is smaller for lower ice temperature. That is to say, ice is less ductile for lower temperature.

Effect of Ice Temperature on the Compressive Strength and Modulus

It can be seen from **Table 1** that the compressive strength of ice distributes from 0.36 to 3.67 MPa when ice temperature varies

TABLE 1 | Test results of uniaxial unconfined compressive strength of ice.

Test number	T_{ice} (°C)	L (mm)	L/D	Peak load (Kn)	P_{ice} (MPa)	E_C (MPa)
1	−0.7	38.6	0.38	2.94	0.36	11.7
2	−2.0	41.3	0.40	9.93	1.22	27.5
3	−2.3	42.8	0.42	13.08	1.60	41.7
4	−2.6	39.5	0.39	13.89	1.70	50.1
5	−3.2	40.6	0.40	12.91	1.58	65.3
6	−3.6	42.3	0.41	15.69	1.92	70.2
7	−3.8	41.1	0.40	18.35	2.25	75.7
8	−4.0	40.2	0.39	15.85	1.94	82.7
9	−4.5	40.5	0.40	18.80	2.30	126.7
10	−4.6	41.3	0.40	17.20	2.11	168.1
11	−4.8	38.4	0.38	17.45	2.14	157.9
12	−5.0	41.4	0.41	23.21	2.84	181.8
13	−5.2	42.0	0.41	20.18	2.47	260.1
14	−5.8	39.5	0.39	24.07	2.95	305.9
15	−6.3	40.7	0.40	26.56	3.25	337.4
16	−7.5	39.6	0.39	29.99	3.67	359.1

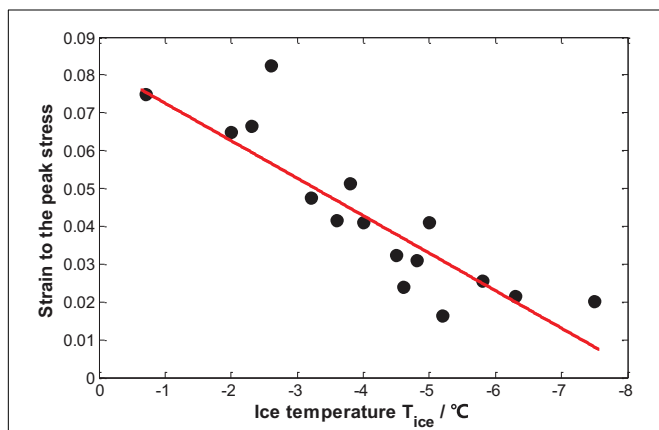L is the ice thickness, mm; D is the diameter of ice specimen, mm.

FIGURE 8 | Relationship between ice temperature and failure strain of ice.

from −0.7 to −7.5°C. The scatter diagram is plotted to illustrate the relationship between ice failure strength and ice temperature (**Figure 9**). The expression to approximate the relationship of the ice failure strength and ice temperature is also obtained through regression and fitting method as shown in Eq. (1).

$$\begin{cases} P_{ice} = -0.4524 T_{ice} + 0.279 \\ R^2 = 0.94 \end{cases} \quad T_{ice} \in [-0.7,\ 7.5] \quad (1)$$

where P_{ice} is the uniaxial unconfined compressive strength of ice (MPa) and T_{ice} is the ice temperature (°C). Eq. (1) shows the good linear relationship between compressive strength and ice temperature, and the correlation coefficient is 0.94. It agrees well with the test results obtained by Wang et al. (2007) and Zhang L. M. et al. (2009). Therefore, the results obtained in the laboratory test will help the mechanical deicing equipment to apply appropriate force on the pavement with ice. That is to say, the force can crush the ice on the one hand and not damage the pavement on the other hand.

In addition, the compressive modulus of ice distributes from 11.7 to 395.1 MPa when ice temperature varies from −0.7 to −7.5°C. The scatter diagram is plotted to illustrate the relationship between ice compressive modulus and ice temperature (**Figure 10**). The approximate expression of the relationship between ice compression modulus and ice temperature is obtained through a regression and fitting method as shown in Eq. (2).

$$\begin{cases} E_C = 7.97 \exp(-0.6233 T_{ice}) & T_{ice} \in [-5,\ 0] \\ R^2 = 0.97 \\ E_C = 365.5 - 0.15 \left(-\dfrac{T_{ice}}{10}\right)^{-10.2} & T_{ice} \in [-8,\ -5] \\ R^2 = 0.97 \end{cases} \quad (2)$$

where E_C is the uniaxial unconfined compressive modulus of ice (MPa).

As can be seen from Eq. (2), when the ice temperature is higher than −5°C, the relationship between ice compression modulus
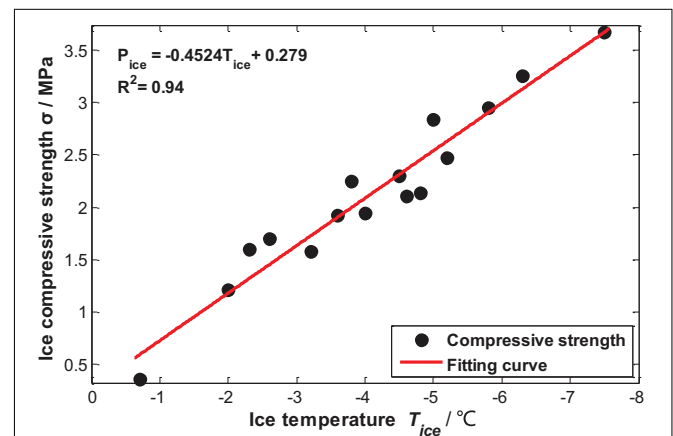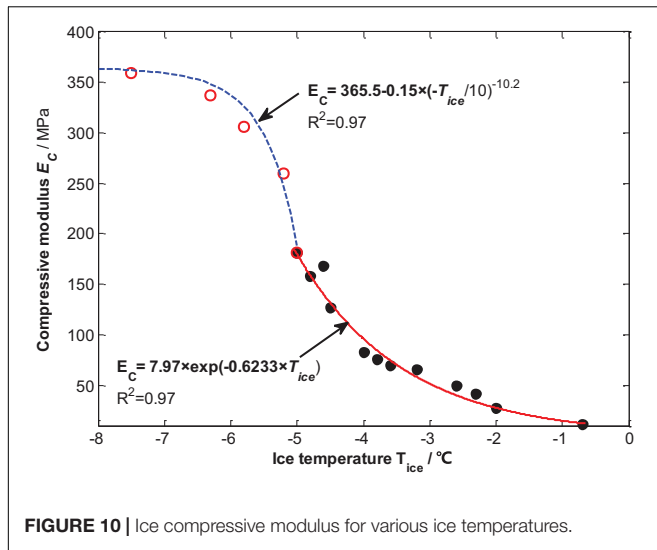

FIGURE 9 | Uniaxial unconfined compressive strength of ice for various temperatures.

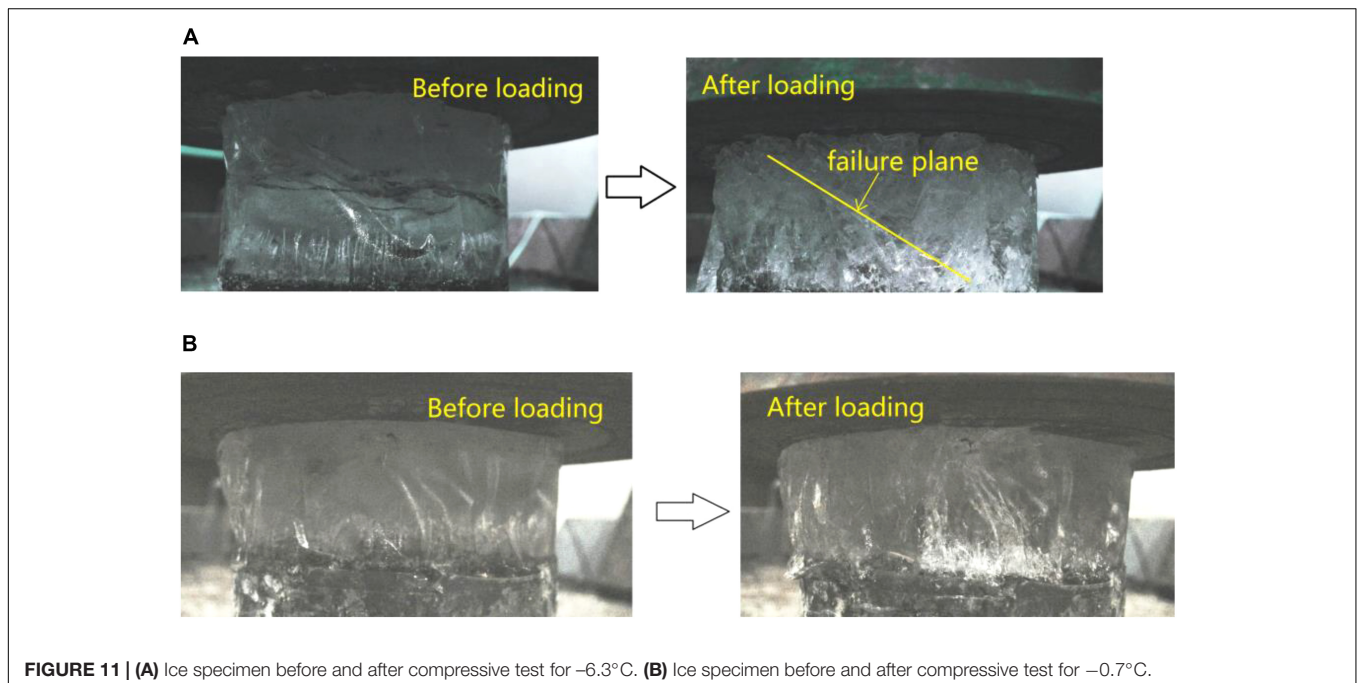FIGURE 10 | Ice compressive modulus for various ice temperatures.

results can provide the value of compressive modulus of ice to facilitate the calculation in simulating the mechanical behavior of material and structure including ice layer.

Ice Failure Mode Under Different Temperature Conditions

According to some researches (Sinha, 1981; Timco and Frederking, 1982; Petrovic, 2003; Zhang X. Z. et al., 2009), ice failure mode depends on strain rate (i.e., load speed) and is affected by ice temperature as well. It can be found that the failure behaviors during the test process are obvious different for various ice temperatures.

Figures 11A,B show the schematic diagrams of ice failure subjected to load at −6.3 and −0.7°C respectively. When ice temperature is −6.3°C, the visible cracks from top to bottom in the ice specimen develop quickly and connect gradually, accompanied by a crisp crush sound during the loading process. Significantly, it can be found from **Figure 11A** that an approximately incline failure plane (not accurate failure plane) appears and the ice particle partially moves along the plane, which can be observed. This phenomenon is regarded as ice shear failure. Because no lateral confinement is applied to the ice cylinder, the ice cylinder expands laterally and is compressed vertically. The obvious peak stress value can be obtained from the stress–strain curve (**Figure 7**) and the failure ice is mainly composed of large ice strips and bulks (**Figure 12A**).

While the failure phenomenon of ice at −0.7°C is inconsistent with that of ice at −6.3°C. Under this condition, ice cylinder is compressed vertically and expands laterally in the process of loading and does not have obvious failure plane like that at −6.3°C (**Figure 11B**). It can be seen from the **Figure 12B**
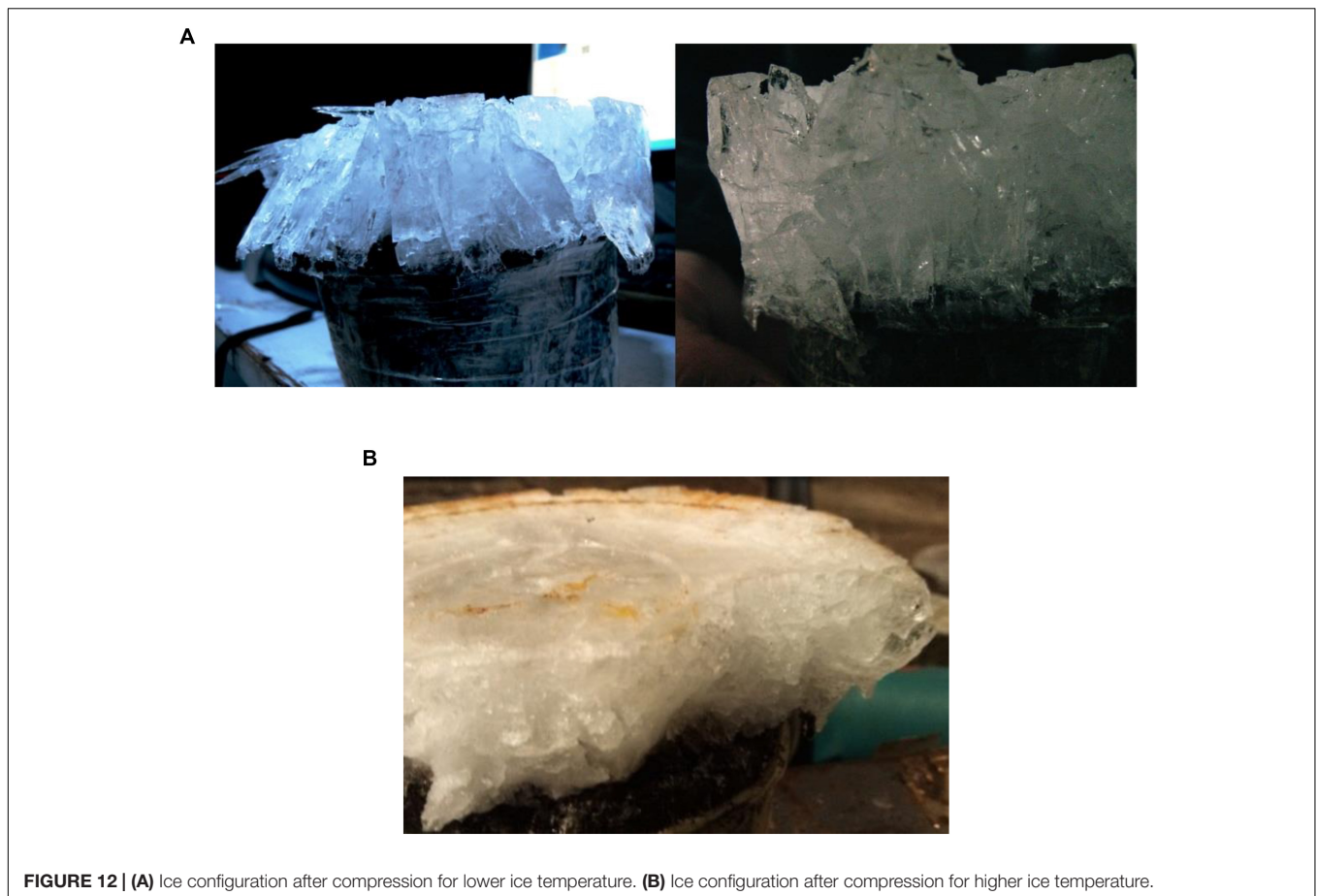
and ice temperature is approximately exponential, and the correlation coefficient is 0.97. When the ice temperature ranges from −8 to −5°C, this kind of relationship can be approximated by power function, and the correlation coefficient is 0.97.

It can be seen apparently from **Figure 10** that the compression modulus improves with ice temperature decrease. The improvement tends to be gentle when ice temperature approaches −10°C. According to other researchers (Wang et al., 2007; Yu et al., 2009), the improvement of compressive modulus with ice temperature is slight when ice temperature is below −10°C, and it is affected by ice strain rate. Since the laboratory condition is limited, the compressive test is not conducted for lower ice temperature (below −10°C). Nevertheless, the test

FIGURE 11 | **(A)** Ice specimen before and after compressive test for −6.3°C. **(B)** Ice specimen before and after compressive test for −0.7°C.

FIGURE 12 | (A) Ice configuration after compression for lower ice temperature. **(B)** Ice configuration after compression for higher ice temperature.

that the failure ice is mainly composed of granular ice crystals, which is different from that of ice under the lower-temperature condition.

General conclusions can be drawn from the above experiment phenomenon, namely, that the failure mechanism of ice on the asphalt pavement under relatively lower temperature is due to the development of cut-through cracks inside the ice. The ice crack development results in the decline of ice-bearing capacity until it reaches whole failure state. The apparent failure plane inside the ice appears and no melting phenomenon can be observed. In contrast, for ice with relatively higher temperature especially the ice near melting point temperature, the visible cracks are less developed.

CONCLUSION

The uniaxial unconfined compressive tests of ice under different cold temperature conditions are carried out. With the aid of a data acquisition system, the load–displacement curves and stress–strain curves of each test are obtained and the test results are analyzed. Accordingly, the experimental conclusions can be drawn as follows:

(1) The different positions that peak stress occurs in the stress–strain curves illustrate that the deformation properties of

ice under various temperatures are not the same. Overall, the strain is smaller for the lower ice temperature. It indicates that the ice is less ductile for lower temperature.

(2) The uniaxial unconfined compressive strength of ice is evaluated, and it distributes from 0.36 to 3.67 MPa when the ice temperature varies from -0.7 to $-7.5°C$. The relation of ice failure strength and ice temperature can be approximately evaluated in a linear manner. The strength can help the mechanical deicing equipment to apply appropriate force on the pavement with ice. That is to say, the force can crush the ice on the one hand and not damage the pavement on the other hand.

(3) The compressive modulus of ice distributes from 11.7 to 359.1 MPa when the ice temperature ranges from -7.5 to $-0.7°C$. The expression to approximate the relation of ice compressive modulus and ice temperature is obtained through a regression and fitting method. It shows good power function and exponential relationships, respectively, when ice temperature ranges from -8 to $-5°C$ and from -5 to $0°C$. The test results can provide the value of compressive modulus of ice to facilitate the calculation in simulating the mechanical behavior of material and structure including ice layer.

(4) The failure mechanism of ice under relatively lower temperature is due to the crack development of

cut-through cracks inside the ice. The ice crack development results in the decline of ice-bearing capacity until it reaches a whole failure state. The relatively apparent failure plane inside the ice can be formed and no melting phenomenon can be observed. In view of the low strain rate, the ice failure mode for this kind of condition is shear failure and ductile, and the failure ice is mainly composed of large ice strips and bulks.

(5) For ice with relatively higher temperature especially the ice near the melting point temperature, the visible cracks are less developed. In view of the low strain rate, the ice failure mode is compressive and ductile, and the failure ice is mainly composed of granular ice crystals.

DATA AVAILABILITY STATEMENT

The raw data supporting the conclusions of this article will be made available by the authors, without undue reservation, to any qualified researcher.

AUTHOR CONTRIBUTIONS

HD and YR designed the experiments. DX carried out the experiments. WL and RZ analyzed the experimental results. WL and HD wrote the manuscript. All authors contributed to the article and approved the submitted version.

FUNDING

REFERENCES

Chen, W., Du, X. H., and Wang, D. L. (2008). Analysis of the low temperature, ice- snow and freezing disasters in early 2008. *Sci. Meteorol. Sin.* 28(Suppl.), 84–87.

Croutch, V. K., and Harttey, R. A. (1992). Adhesion of ice to coatings and the performance of ice release coatings. *J. Coat. Technol.* 64, 41–52.

Dan, H. C., He, L. H., Zou, J. F., Zhao, L. H., and Bai, S. Y. (2014). Laboratory study on the adhesive properties of ice to the asphalt pavement of highway. *Cold Reg. Sci. Technol.* 104, 7–13. doi: 10.1016/j.coldregions.2014. 04.002

Dan, H. C., Tan, J. W., and Chen, J. Q. (2019a). Temperature distribution of asphalt bridge deck pavement with groundwater circulation temperature control system under high- and low temperature conditions. *Road Mater. Pavem. Des.* 20, 528–553.

Dan, H. C., Zhang, Z., Liu, X., and Chen, J. Q. (2019b). Transient unsaturated flow in the drainage layer of a highway: solution and drainage performance. *Road Mater. Pavem. Eng.* 20, 528–553. doi: 10.1080/14680629.2017.139 7049

Dan, H. C., Tan, J. W., Du, Y. F., and Cai, J. M. (2020a). Simulation and optimization of road deicing salt usage based on Water-Ice-Salt model. *Cold Reg. Sci. Technol.* 169:102917. doi: 10.1016/j.coldregions.2019. 102917

Dan, H. C., Yang, D., Liu, X., Peng, A. P., and Zhang, Z. (2020b). Experimental investigation on dynamic response of asphalt pavement using SmartRock sensor under vibrating compaction loading. *Constr. Build. Mater.* 247:118592. doi: 10.1016/j.conbuildmat.2020.118592

Dan, H. C., Zou, Z. M., Zhang, Z., and Tan, J. W. (2020c). Effects of aggregate type and SBS copolymer on the interfacial heat transport ability of asphalt mixture using molecular dynamics simulation. *Constr. Build. Mater.* 250:118922. doi: 10.1016/j.conbuildmat.2020.118922

Gow, A. J., and Williamson, T. C. (1972). Linear compressibility of ice. *J. Geophys. Res.* 77, 6348–6352. doi: 10.1029/jb077i032p06348

Gustafson, K. (1982). Icing conditions on different pavement structures. *Transp. Res. Rec.* 860, 21–28.

Hanbali, R. M. (1994). Economic impact of winter road maintenance on road users. *Transp. Res. Rec.* 1442, 151–161.

Haynes, F. D., and Mellor, M. (1977). Measuring the uniaxial compressive strength of ice. *J. Glaciol.* 19, 213–223. doi: 10.3189/s0022143000029294

Kärnä, T., and Jochmarm, P. (2003). "Field observations on ice failure modes", in *Proceedings of the 17th POAC Symposium on Ice*. Trondheim Norway: POAC International Committee.

Kärnä, T., Lubbad, R., Løset, S., Mroz, A., Dalane, O., Bi, X., et al. (2010). "Ice failure process on fixed and compliant cones," in *Proceedings of the HYDRALAB III Joint User Meeting*, Hannover, 1–4.

Marion, G. M., and Jakubowski, S. D. (2004). The compressibility of ice to 2.0 kbar. *Cold Reg. Sci. Technol.* 38, 211–218. doi: 10.1016/j.coldregions.2003. 10.008

Montagnat, M., Castelnau, O., Bons, P. D., Faria, S. H., Gagliardini, O., Gillet-Chaulet, F., et al. (2014). Multiscale modeling of ice deformation behavior. *J. Struc. Geol.* 61, 78–108. doi: 10.1016/j.jsg.2013.05.002

Oksanen, P. (1983). *Friction and Adhesion of Ice*. Espoo: Technical Research Centre of Finland, Publication, 36.

Petrenko, V. F. (1999). Reduction of ice adhesion to stainless steel by ice electrolysis. *J. Appl. Phys.* 86, 5450–5454. doi: 10.1063/1.371544

Petrovic, J. J. (2003). Review mechanical properties of ice and snow. *J. Mater. Sci.* 38, 1–6. doi: 10.1023/A:1021134128038

Sarkar, D. K., and Farzaneh, M. (2009). Superhydrophobic coatings with reduced ice adhesion. *J. Adhes. Sci. Technol.* 22, 1215–1237. doi: 10.1163/156856109x433964

Schulson, E. M. (2001). Brittle failure of ice. *Eng. Fract. Mech.* 68, 1839–1887. doi: 10.1016/S0013-7944(01)00037-6

SHRP (1994). *). Development of Anti-Icing Technology*. Washington, D.C: SHRP - National Research Council. SHRP-H-385.

Sinha, N. K. (1981). Rate sensitivity of compressive strength of columnar-grained ice. *Exp. Mech.* 21, 209–218. doi: 10.1007/bf02326843

Sodhi, D. S. (2001). Crushing failure during ice–structure interaction. *Eng. Fract. Mech.* 68, 1889–1921. doi: 10.1016/s0013-7944(01)00038-8

Taggart, D. G., Osama, I., and Milton, H. (2002). Application of jetting technology to pavement deicing. *Transp. Res. Rec.* 1794, 77–83. doi: 10.3141/1794-10

Tan, Y. Q. (2008). Deicing technologies for the pavement in the ice disaster. *Trans. Constr. Manag.* 49, 86–87.

Timco, G. W., and Frederking, R. M. W. (1982). Comparative strengths of fresh water ice. *Cold Reg. Sci. Technol.* 6, 21–27. doi: 10.1016/0165-232x(82)90041-6

Wang, J. F., Yu, T. L., and Huang, M. L. (2007). Experimental research on uniaxial and unconfined compressive strength of river ice. *Low Temp. Archit. Technol.* 1, 11–13.

Weertman, J. (1983). Creep deformation of ice. *Annu. Rev. Earth Plane. Sci.* 11, 215–240. doi: 10.1146/annurev.ea.11.050183.001243

Yu, T. L., Yuan, Z. G., and Huang, M. L. (2009). Experimental study on mechanical behavior of river ice. *J. Liaon. Techn. Univ.* 28, 937–940.

Yurtseven, H., and Kilit, E. (2009). Calculation of the compressibility and heat capacity of ice I in the pre-melting region. *Phys. Chem. Liquids* 47, 495–504. doi: 10.1080/00319100802290449

Zhang, D. C., Liu, M. Y., and Bao, T. (2011). Experimental study on mechanical properties of fresh water ice subjected to uniaxial compressive load. *Eng. Mech.* 28, 238–244.

Zhang, L. M., Li, Z. J., and Jia, Q. (2009). Experimental study on uniaxial compressive strengths of artificial freshwater ice. *J. Hydraul. Eng.* 40, 1392–1396.

Zhang, X. Z., Bai, R. Y., and Jiang, A. M. (2009). Constitutive relation and compressive strength of oceanic ice. *Mech. Eng.* 31, 50–53.

Zhu, Y. S., Xiang, H. L., and Zhang, X. D. (2012). The skid resistance performance of the asphalt pavement under freezing condition. *J. Wuhan Univ. Technol.* 36, 6–10.